JOURNAL OF MATERIALS SCIENCE **40** (2005) 6473–6481

Tool penetration during friction stir spot welding of Al and Mg alloys

A. GERLICH, P. SU, T. H. NORTH
Department of Materials Science and Engineering, University of Toronto, Toronto, Ontario, Canada

Published online: 5 October 2005

The mechanism of tool penetration during friction stir spot welding of Al-alloy and Mg-alloy sheet materials is investigated and is explained as a progression of wear events, from mild wear to severe wear and then to melt wear in material beneath the base of the rotating pin. Melt wear can also occur under the rotating tool shoulder provided that sufficient penetration of the upper sheet occurs during the spot welding operation.

The highest temperatures attained during FSW spot welding of Al 6111 and AZ91 base materials are close to the solidus temperatures of each base material and correspond with $0.94T_s$ (Al 6111) and 0.99 T_s (AZ91) where T_s is the solidus temperature of the material in degrees Kelvin.

1. Introduction

Friction stir spot welding (FSSW) is a process variant of friction stir welding, which produces joints by plunging a rotating tool comprising a pin and a shoulder into two sheets and then retracting the tool leaving a keyhole depression. Plasticized material formed at the periphery of the keyhole facilitates joint formation between the contacting sheets [1, 2]. Tool penetration is generally disregarded in the published research on friction stir welding since it only represents the initial 'touchdown' stage in the joining operation. However, since the whole FSSW operation typically lasts from two seconds to a maximum of five seconds, the process of tool penetration essentially determines heat generation, plasticized material formation around the rotating pin, joint formation and weld mechanical properties.

The relative contributions made by the pin and the tool shoulder have been the subject of debate during friction stir welding, with investigators suggesting that heat generation under the much larger diameter tool shoulder is the dominant feature [3, 4]. However, the pin and shoulder regions play quite different roles during FSSW since the tool shoulder comes into contact with the upper sheet surface late in the spot welding operation and only after the rotating pin has completely penetrated the upper sheet and begun to penetrate the lower sheet. It is shown later that the tool shoulder only begins to play an important role in the joining operation when material extruded from the keyhole becomes trapped between the surface of the upper sheet and the tool shoulder. From this point onward the tool shoulder provides both frictional heating and compressive loading, which facilitates joint formation between the two contacting sheet materials.

The present paper details some of the results of a wide-ranging program, which is investigating friction stir spot welding of Al-alloy and Mg-Alloy base materials for automotive applications [5–8]. A combination of data acquisition of key welding parameters (axial force, torque and tool displacement), high-speed imaging, temperature measurement and metallography are employed. It is shown that tool penetration can be explained as a progression of wear events from mild (delamination) wear, through to severe wear, and finally to melt wear in the plasticized material immediately under the base of the rotating pin.

2. Experimental procedure

The sheet materials employed during FSSW trials comprised 1.5 mm thick AZ91D, Al 6061-T6 and Al 5754-H12 and 1.3 mm thick Al 6111-T4. The test specimen dimensions were 25 × 100 mm in all cases. The FSW welding equipment provided rotational speeds from 1000 to 3000 RPM and axial loads up to 12 kN (2800 lb-f). The plunge rate during FSW spot welding ranged from 0.1 to 10 mm/s with the penetration depth controllable to ±0.1 mm. FSW spot welding was carried out using an H13 steel tool, which had a hardness of 46–48 HRc, a shoulder diameter of 10 mm, a pin diameter of 4 mm and a pin length of 2.2 mm. A smooth (unthreaded) tool without a shoulder was employed during some spot welding trials and in this case the pin diameter was 4 mm.

The axial load and the torque values were measured using a JR3 six-axis load cell, which was coupled with a data acquisition system so that axial force, torque, penetration depth and temperature outputs during spot welding were logged on a desktop computer. Tool displacement (penetration depth) was measured using a linear transducer, which had an accuracy of ±0.01 mm while the spindle RPM was measured using a shaft

0022-2461
DOI: 10.1007/s10853-005-1568-9

encoder, which had an accuracy of ±30 RPM. Synchronous high-speed CCD imaging during friction stir spot welding was accomplished by viewing the weld region side-on using a frame-rate of 250 fps.

During all temperature measurements the FSSW tool was held stationary and the Al-alloy and Mg-alloy test specimens were rotated. 0.25 mm diameter *K*-type thermocouples were located 0.2 mm from the end of the rotating pin and at the mid-radius location on the tool shoulder. The thermocouples were inserted into 1.0 mm diameter holes in the tool assembly so that the tips of the thermocouple were in direct contact with plasticized material formed during the FSW spot welding operation. A separate A/D converter collected temperature output in degrees Celsius and enabled synchronous measurement of axial force, torque, tool displacement and temperature during FSW spot welding. The plunge rates were 1.0 to 2.5 mm/s during temperature measurement and a four second dwell period was incorporated into spot welding cycle during which tool rotation continued. Unless otherwise stated all temperature measurements were repeated at least twice. During repeat testing the average measured temperature was within ±5°C of that indicated in each figure.

During metallographic examination the Al-alloy weld sections were etched using Keller's reagent, while the Mg-alloy test sections were etched using acetic-picral solution comprising 10 ml acetic acid, 4.2 g picric acid, 10 ml H_2O and 70 ml of 95% ethanol.

3. Results

Figs 1 and 2 show the axial force, torque and tool displacement (penetration depth) outputs produced during spot welding of Al 6111 and AZ91 sheets. Two peaks (F_1 and F_2) are exhibited in the axial force output. When the FSW spot welding process initiates the axial force increases until the F_1 peak is reached and then decreases. Both the axial force and torque increase again following the F_1 peak and the welding operation ends when the F_2 peak is attained.

Figs 3 and 4 show thermal cycles produced at the base of the rotating pin and at the mid-radius location on the tool shoulder during spot welding of Al 6111 and AZ91. The highest temperatures at the base of the pin are 532°C (Al 6111) and 462°C (AZ91D). Lower temperatures are produced at the tool shoulder region, namely 480°C (Al 6111) and 437°C (AZ91).

Figs 5a–c show the results produced during high-speed imaging of the FSW spot welding process. The arrow markings in these figures show the correspondence between the high speed imaging output and axial force and torque values as the spot welding operation proceeds. Debris was ejected during tool penetration of both Al 6111 and AZ91 base materials. Fig. 6 shows debris, which is ejected when the rotating pin penetrates into Al 6111 and AZ91 sheet material. Some Al 6111 debris was highly deformed and had serrated edges (Fig. 6a and b) while AZ91 debris exhibited a densely layered (feathery) morphology (Fig. 6c and d).

4. Discussion

The FSW spot welding process initiates when the rotating pin moving at a given plunge rate contacts the surface of the upper sheet and the axial force and the torque values start to increase. It has already been shown that mild wear occurs when a pressure of 1.0 MPa is exerted by SAE 52100 steel counterface as it slides at a velocity of 0.4 m/s over Al 6061-T6 base material [9]. Mild wear is characterized by plastic shearing and the nucleation and propagation of subsurface cracks which reach the surface, creating wear debris [9–11]. The cross-sectional area at the base of the pin is 11.47 mm^2 during FSW spot welding using a 4 mm diameter pin.

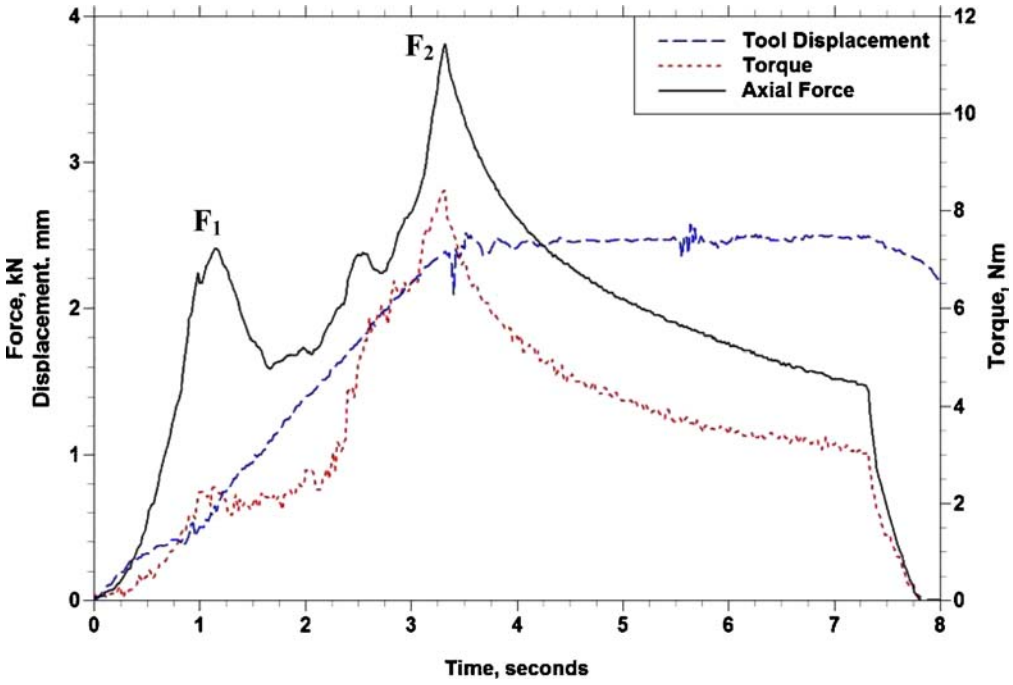

Figure 1 Axial force, tool displacement and torque outputs during FSW spot welding of Al 6111 base material.

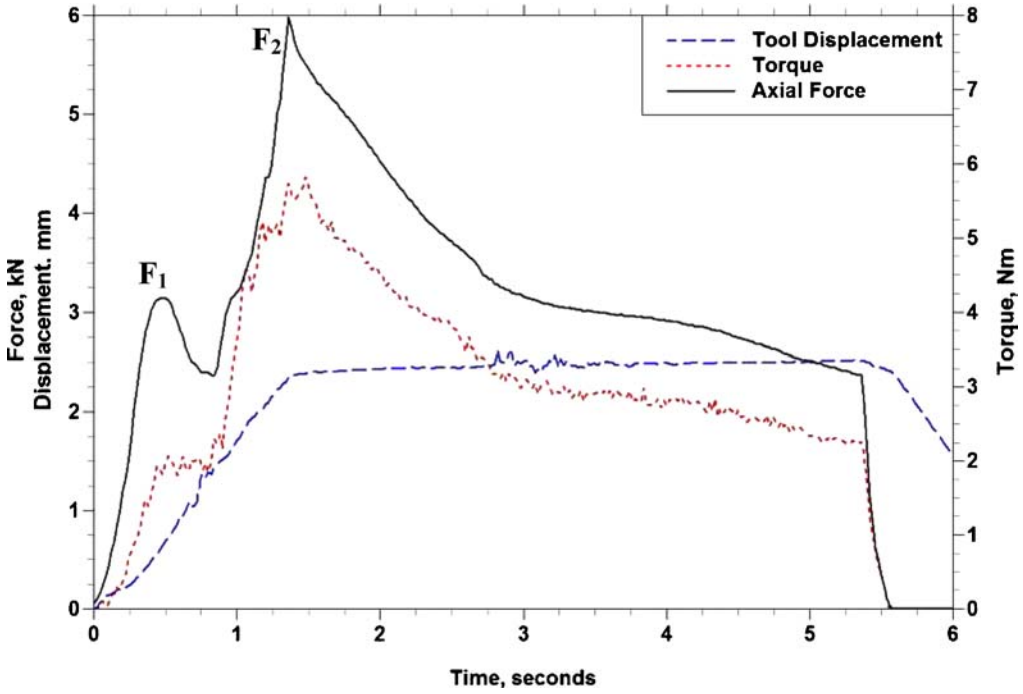

Figure 2 Axial force, tool displacement and torque outputs during FSW spot welding of AZ91 base material.

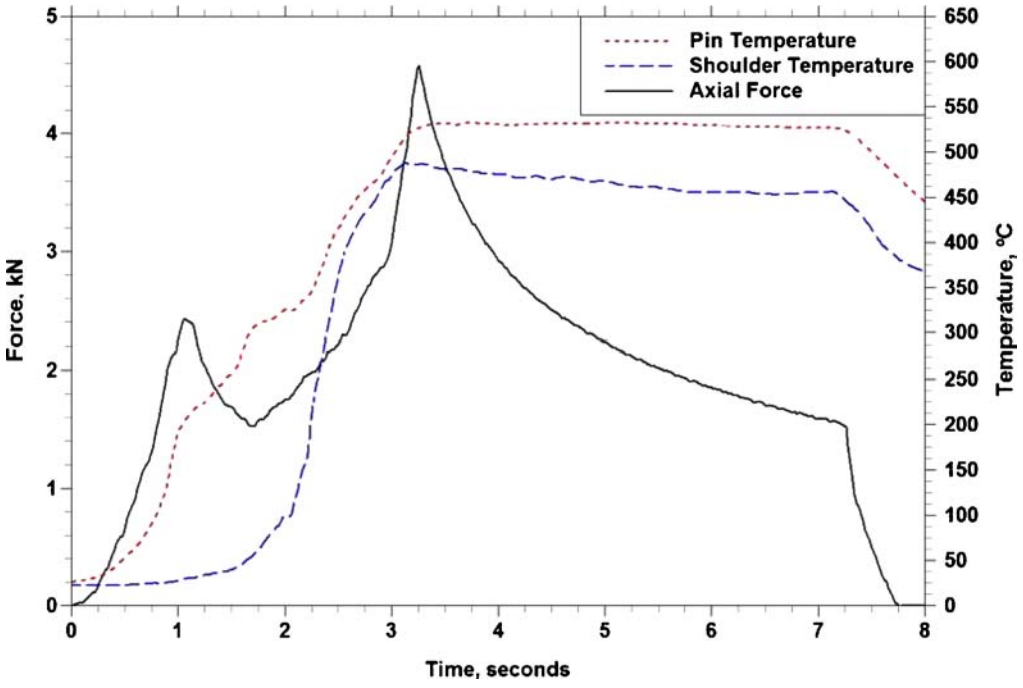

Figure 3 Temperature output during FSW spot welding of Al 6111 base material.

Therefore it would be expected that mild wear would initiate immediately beneath the rotating pin when the axial load is less than 11.47 N. Fig. 1 shows that the axial load exceeds 11.47 N very early in the spot welding operation, e.g. when the penetration depth into Al 6111-T4 base material is less than 100 μm. Considering that the hardness of Al 6111-T4 is lower than that of Al 6061-T6, the initiation of mild wear would be inevitable at this early stage of penetration. Similarly, based on sliding wear testing results reported by Chen and Alps using AZ91 magnesium base material [10] mild wear will occur very early during spot welding of this base material. Fig. 7 provides support for this contention since the delamination formed during the first 75 μm of penetration into AZ31 magnesium base material is a characteristic feature of mild wear [9–12].

As the tool penetration process continues there will be a transition from mild to severe wear. Zhang and Alpas [9] found that the transition from mild to severe wear occurred when a pressure of only 10.0 MPa was exerted by an SAE 52100 steel sliding over Al 6061 base material at a velocity of 0.4 m/s. The weighted average tangential velocity at the base of the 4 mm diameter pin is 0.418 m/s during FSW spot welding using a rotational speed of 3000 RPM. Consequently, the pressure beneath the rotating pin will be 10 MPa when the axial the load reaches 114.7 N, a value exceeded

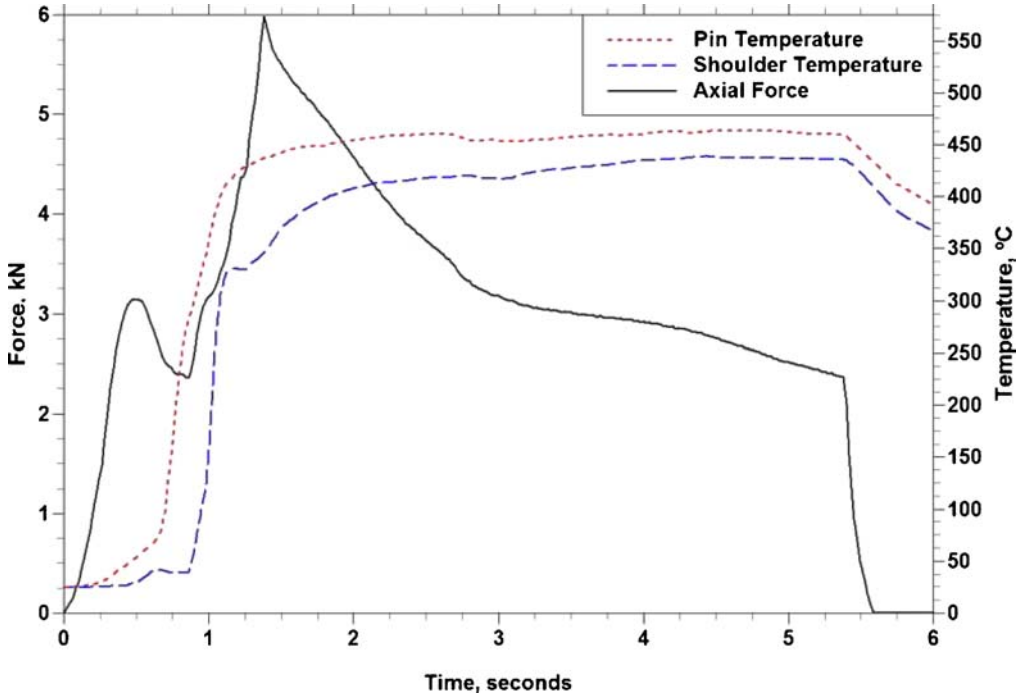

Figure 4 Temperature output during FSW spot welding of AZ91 base material.

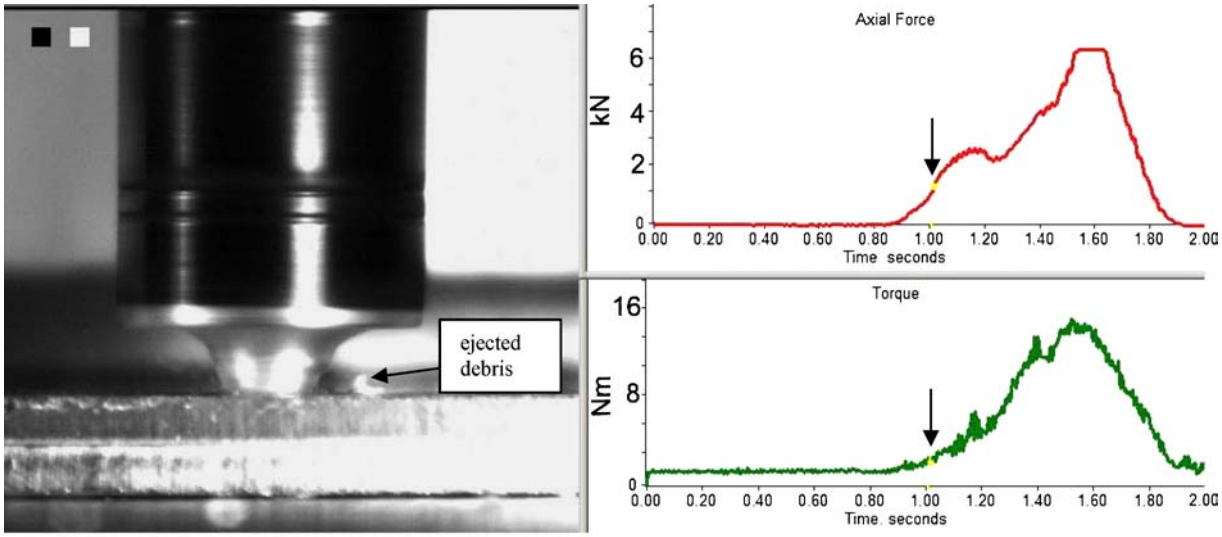

(a)

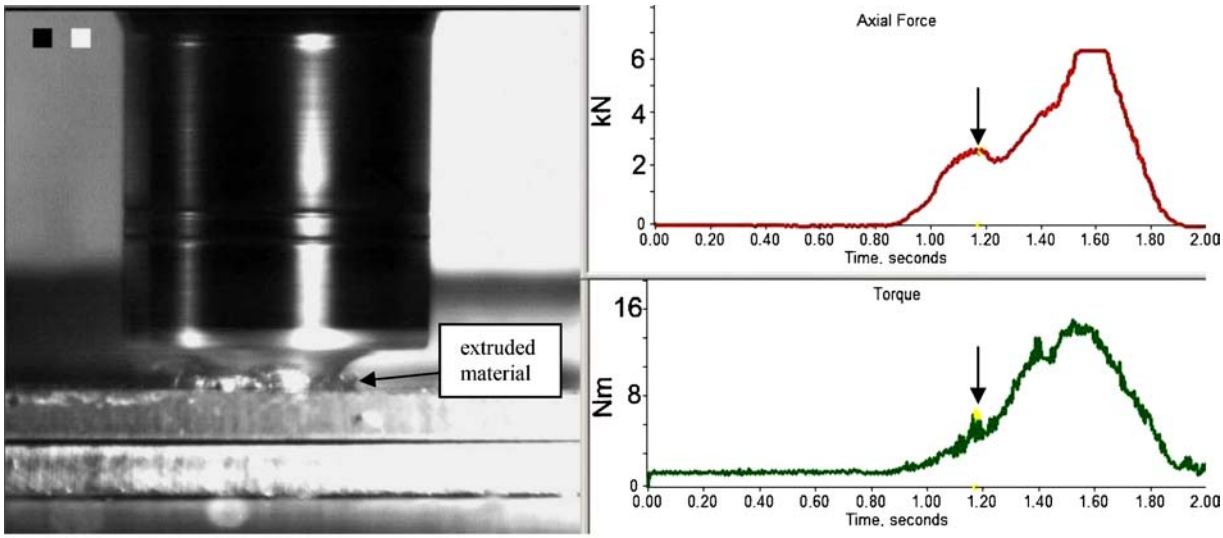

(b)

Figure 5 (a–c) Synchronous high-speed imaging and axial force and torque output during FSW spot welding of Al 5754 base material.

(*Continued*)

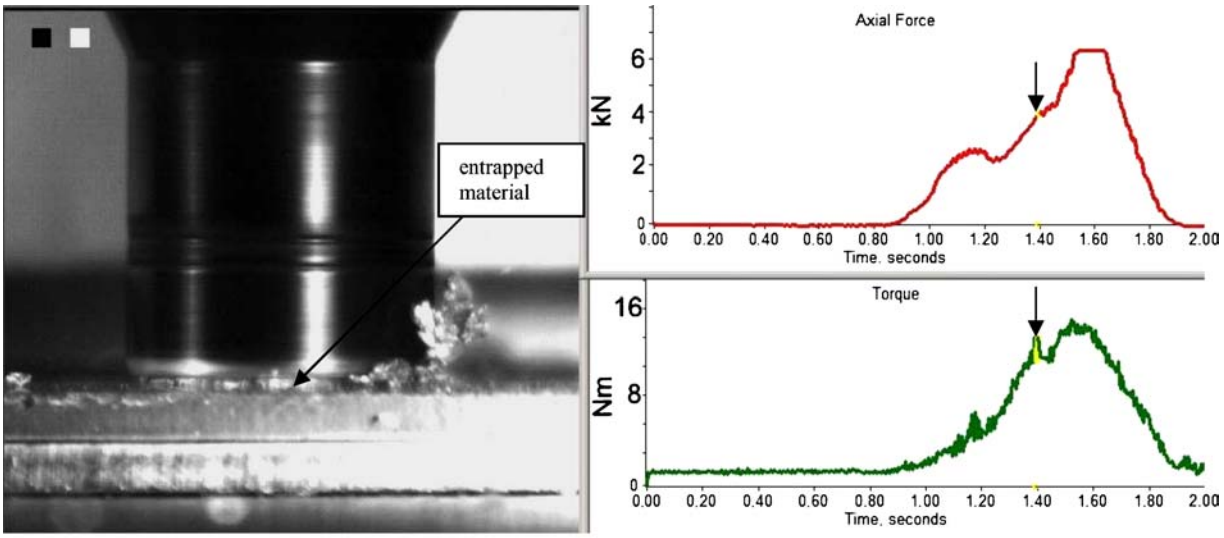

(c)

Figure 5 (*Continued*)

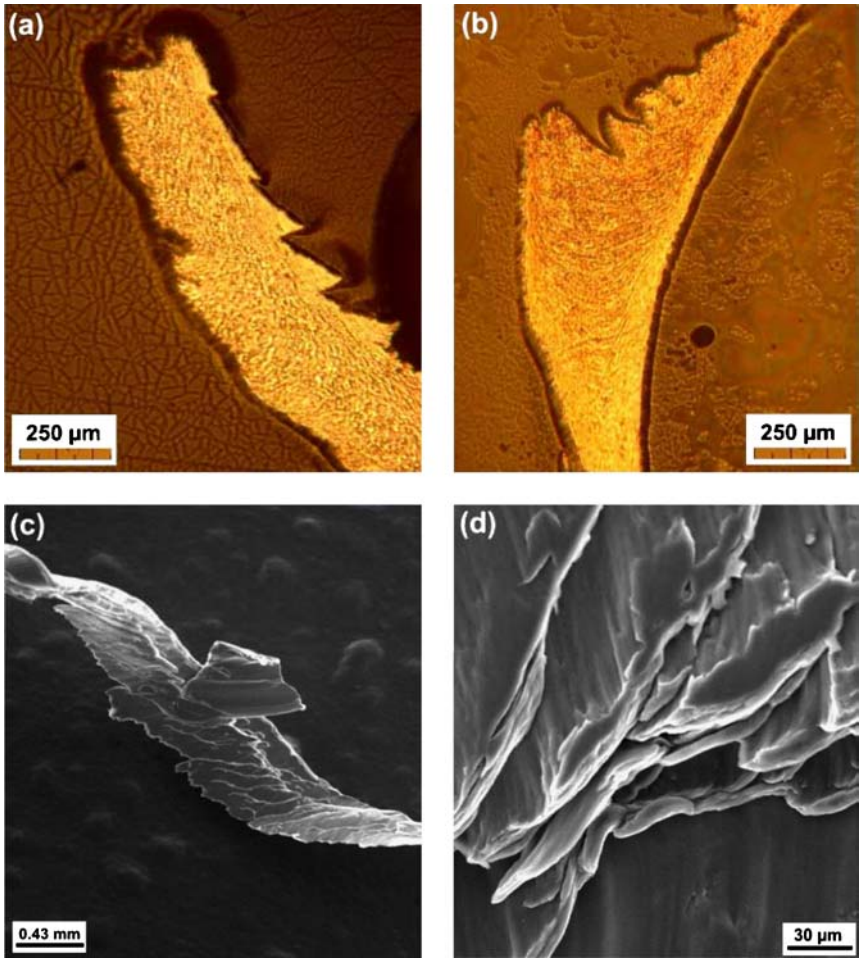

Figure 6 (a & b) Optical micrographs of wear debris ejected during penetration of Al 6111 base material. (c & d) SEM images of wear debris ejected during penetration of AZ91 base material.

during the first 50 ms when Al 6111 base material is welded, see Fig. 1. When the base of the rotating pin is completely enveloped in the Al 6111 sheet material, the normalized force $\bar{F} = \frac{F}{A_n H_0} = 1$, where A_o is the nominal area of contact at the sliding surface and H_0 is the room temperature hardness of the base material. $\bar{F} = 1$ is the generally accepted requirement for seizure during sliding wear [13].

Severe wear occurs when thermally-activated deformation processes promote softening of material immediately adjacent to the contact interface [9] and therefore the base of the rotating pin becomes coated with an adhering layer of Al 6111 or AZ91 base material. Fig. 8 shows images of the base of the rotating pin at different penetration depths. This output is typical of that produced by adhesion and seizure events, which

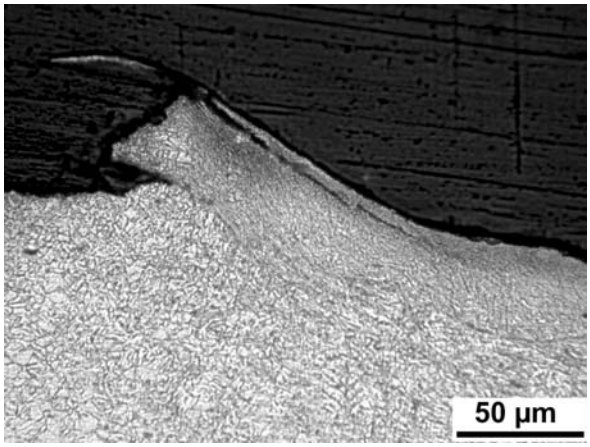

Figure 7 Delamination produced when AZ31 magnesium sheet is penetrated to a depth of 75 μm.

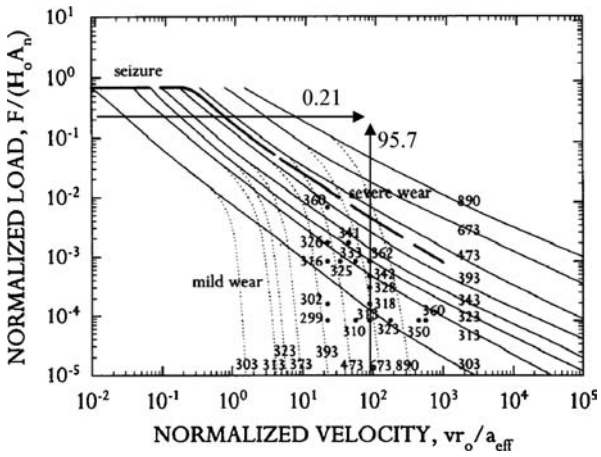

Figure 9 Al 6061/steel wear map (after Zhang and Alpas [9]).

continue until the base of the rotating pin is almost completely covered with an adhering film when the pin reaches a penetration depth of 500 μm in both Al-alloy and Mg-alloy base materials.

Fig. 6 shows examples of wear debris ejected during tool penetration. The wear debris produced during penetration of Al 6111 sheet is highly deformed and shows evidence of cutting by the threads on the rotating pin. In contrast, the AZ91 wear debris has a feathery morphology comprising approx. 10 μm thick material layers. This type of morphology is remarkably similar to the layered structured created when melt wear occurs during sliding wear testing of AZ91 base material [10]. The layered structure is produced when local melted material is repeatedly squeezed out from the contact interface.

It has been suggested that the sudden decrease in axial force following the F_1 peak occurs when melt wear becomes the dominant feature in plasticized material immediately beneath the rotating pin [5]. Melt wear involves local melting of thin (10–20 μm thick) layers, which dramatically lower the viscosity of plasticized material at the contact interface [9–11, 13–16]. Low viscosity plasticized material is displaced to cooler regions where it solidifies due to the pressure applied by the rotating pin. Following displacement viscous dissipation increases the temperature and local melted films are reformed in plasticized material. The axial force falls suddenly during FSW spot welding since lubrication occurs at the contact interface between the rotating pin and the adjacent plasticized material, see Figs 1 and 2.

Fig. 9 shows the wear diagram produced during sliding wear testing of Al 6061 base material using an SAE 52100 steel slider [9]. The axes in this diagram are the normalized force $\bar{F} = \frac{F}{A_n H_0}$ and the normalized velocity $\bar{v} = \frac{vr_o}{a_{\text{eff}}}$ during sliding wear testing, where r_o is the length of the contact area and a_{eff} is mean thermal diffusivity of the aluminum alloy base material and the steel counterface. The normalized load $\bar{F}$ and the normalized velocity $\bar{v}$ values corresponding with the F_1 peak found during FSW spot welding of Al 6061-T6 sheet material are $\bar{F} = 0.21$ and $\bar{v} = 95.7$ respectively. These values are plotted on Fig. 9 and indicate that the conditions required for melt wear formation should exist immediately under the base of the rotating pin.

It must be emphasized that the conditions beneath the rotating pin and the tool shoulder are quite different from those which exist during conventional sliding wear since oxygen is completely excluded during the tool penetration process. It is well-documented that access by oxygen from the atmosphere during sliding wear testing produces a transition from melt wear to oxidative wear so that the wear rate decreases dramatically since oxides have higher melting temperatures and do not flow easily [13]. However, oxidative wear cannot occur during tool penetration and melt wear, once initiated, will continue as the dominant wear mechanism, which determines the tool penetration process. Based on this argument, the axial force and the torque should

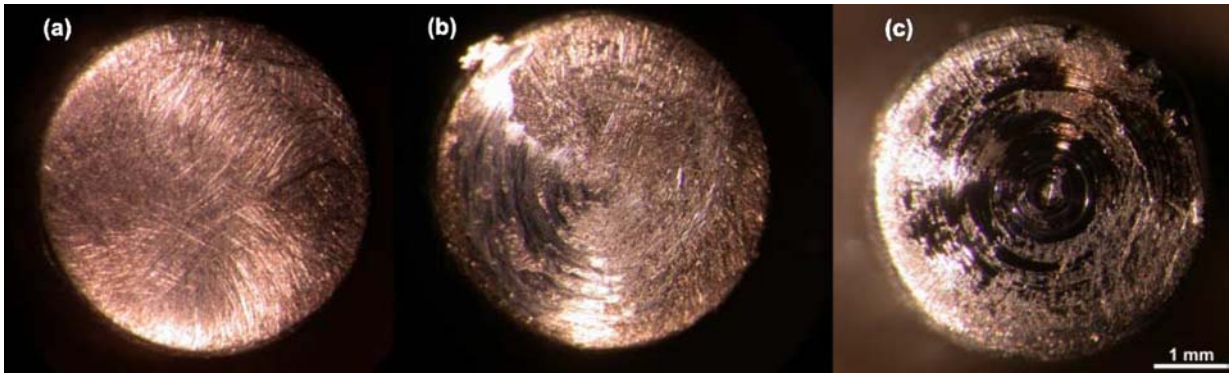

Figure 8 (a) Clean pin prior to spot welding, (b) Following 300 μm penetration of Al 6061, (c) Following 400 μm penetration of AZ91.

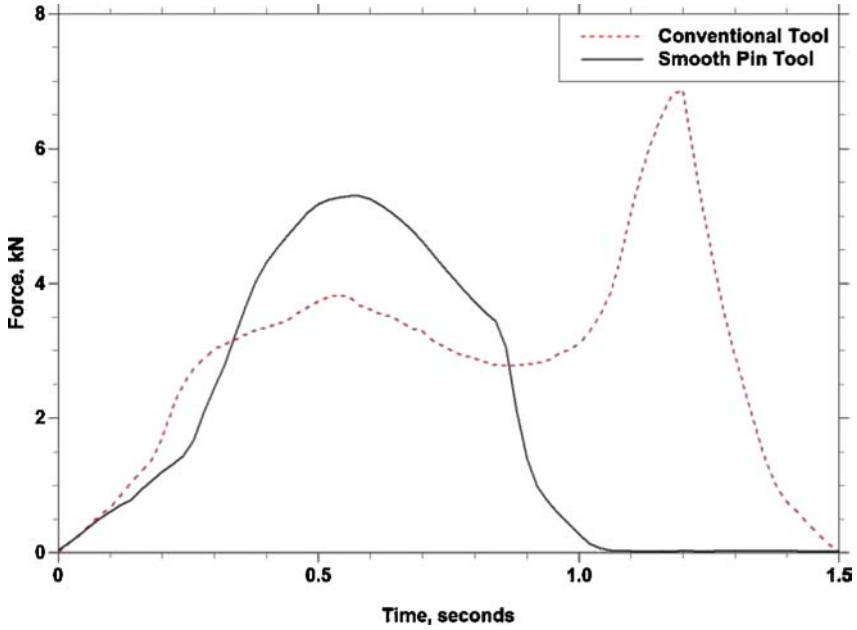

Figure 10 Axial force output produced during spot welding of Al 6061 sheet using a smooth pin tool (without a shoulder) and a conventional tool with a pin and a shoulder.

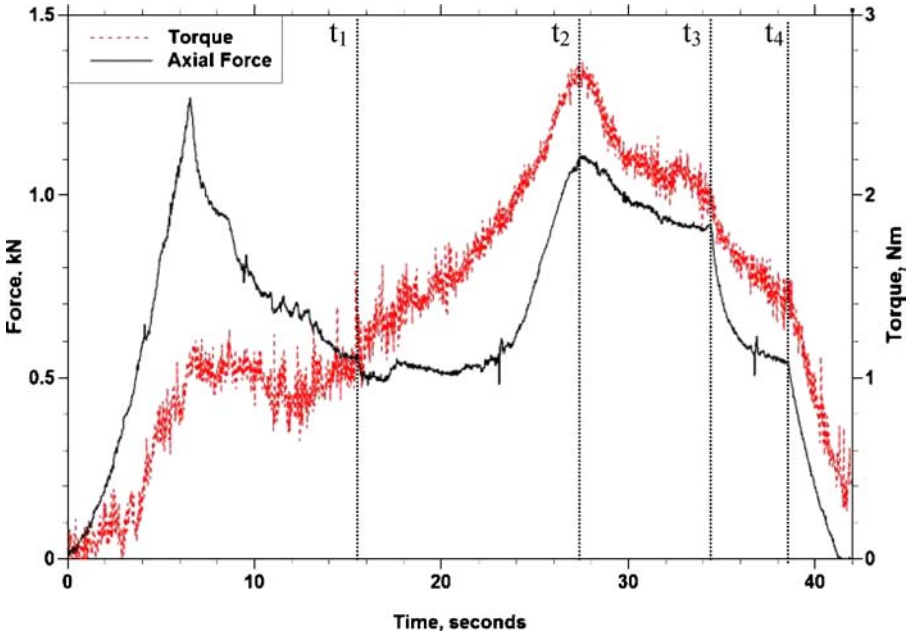

Figure 11 Axial force and torque output during spot welding of Al 6061-T6 sheet using a very slow plunge rate (0.1 mm/s). The tool shoulder begins to contact material extruded from the keyhole at t_1, melt wear under shoulder begins at t_2, while the dwell time is applied from t_3 to t_4.

continue to decrease as the sheet is further penetrated (following the F_1 axial force peak). The results produced during spot welding of Al 6061 sheet material using a smooth (unthreaded) tool without a shoulder support this contention, see Fig. 10. However, it is apparent in Figs 1, 2, 11 and 12 that the axial force and torque values do not continue to decrease following the F_1 peak during spot welding using a conventional tool, which has both a pin and a shoulder. The axial force and the torque increase following the F_1 peak because material extruded from the keyhole region becomes trapped between the tool shoulder and the upper surface of the upper sheet and is forged and plastically deformed before being ejected from the periphery of the tool shoulder, see Fig. 5c.

One would expect that there would be a transition from mild wear to severe wear and then to melt wear in plasticized material beneath the tool shoulder provided that the upper sheet material is sufficiently penetrated during the spot welding operation. Figs 11 and 12 provide support for this assertion. The changes in axial force and in torque during FSW spot welding of Al 6061 and AZ91 base material using an extremely slow plunge rate (0.1 mm/s) are indicated.

The time t_1 in Figs 11 and 12 indicate where the axial force and torque values begin to increase as material extruded from the keyhole is trapped and forged between the tool shoulder and the surface of the upper sheet, see Fig. 5c. The axial force and torque values continue to increase and then suddenly decrease when

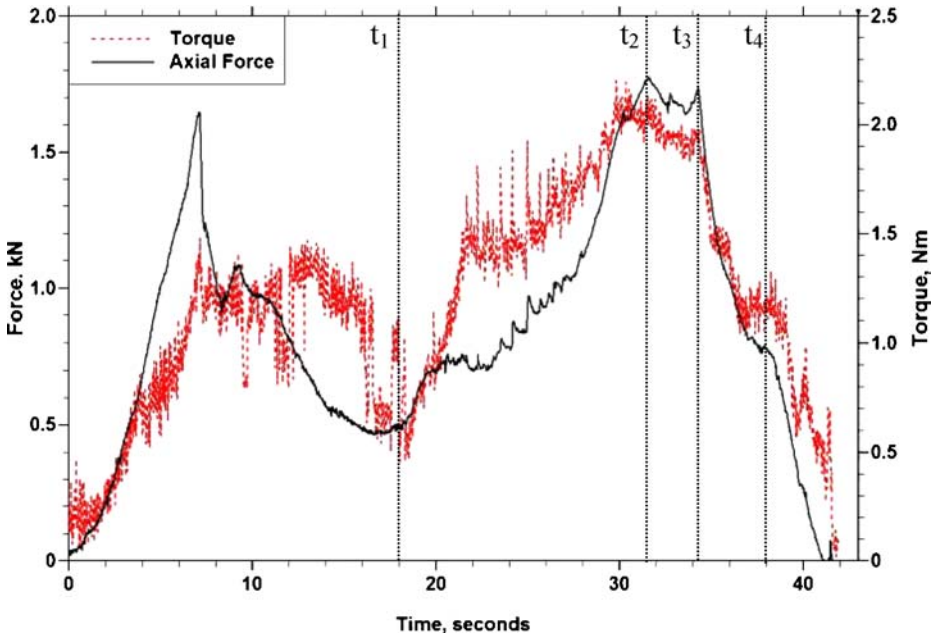

Figure 12 Axial force and torque output during spot welding of AZ91 sheet using a very slow plunge rate (0.1 mm/s). The tool shoulder begins to contact material extruded from the keyhole at t_1, melt wear under shoulder begins at t_2, while the dwell time is applied from t_3 to t_4.

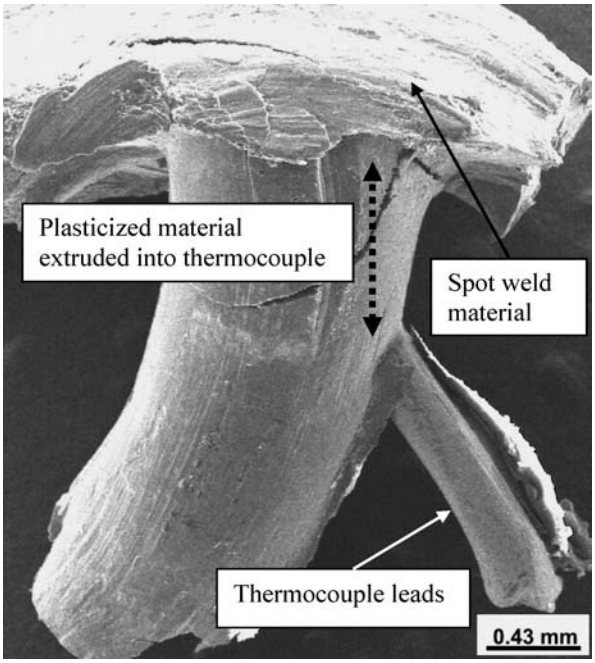

Figure 13 Spot weld material and thermocouple tip removed from tool after temperature measurement.

melt wear occurs. It is possible that the sudden fall and leveling out of axial force and torque values between t_2 and t_3 may be associated with the ejection of local melted material from under the tool shoulder.

5. Temperature output

Figs 3 and 4 show the temperature output measured at the base of the rotating pin and at the mid-radius location on the tool shoulder during FSW spot welding of Al 6111 and AZ91 base materials. The highest temperatures at the base of the rotating pin (532°C in Al 6111 and 462°C in AZ91D) are close to the solidus temperature of each base material. These temperatures correspond with $0.94T_s$ (Al 6111) and $0.99T_s$ (AZ91), where T_s is the solidus temperatures in degrees Kelvin. The highest temperatures reached at the tool shoulder are less than those attained at the base of the rotating pin (480°C in Al 6111 and 437°C in AZ91). However, the measured temperatures at the base of the pin which correspond with the F_1 axial force peaks are approx. 225°C (Al 6111) and 50°C (AZ91), and are much less that the solidus temperature of each base material. At first sight these results appear at variance with the melt wear proposal made earlier in this paper. However, it is important to stress that the thermal output in Figs 3 and 4 indicates the average temperature at the location 0.2 mm from the base of the rotating pin. Also, although the 0.25 mm diameter thermocouples were in direct contact with plasticized material formed during spot welding of Al 6111 and AZ91 their locations were further displaced by up to 0.5 mm when plasticized material was forced into the 1 mm diameter holes in the rotating tool, see Fig. 13.

Since melt wear involves the transient melting, displacement and solidification of 10 μm to 20 μm thick melted layers the region where melt wear occurs will be highly-localized. Bowden *et al.* [15, 16] have pointed out that the temperature decreases dramatically with distance from the contact interface, e.g. during frictional heating of steel samples the contact interface can be as high as 1000°C while the bulk sample remains quite cool. This explains why investigators such as Bowden *et al.* [15, 16] and Quinn *et al.* [17] employed sophisticated measuring techniques when they investigated the peak temperatures generated at contacting interfaces, e.g. involving the combination of e.m.f. measurements with the Seebeck effect [15], infrared photocells [16] and color-temperature calibrations from hot-spot images [17]. Finally, although Chen and Alpas [10] found evidence of melt wear

formation during sliding wear testing of AZ91 base material using an SAE 52100 steel slider the average temperatures measured using thermocouples located within 100 μm of the contacting interface only ranged from 347 K to 585 K. During sliding wear testing of Al 6061 base material the average temperatures measured within 100 mm of the contacting interface were 299 K to 362 K [9].

6. Conclusions

A detailed examination of tool penetration during FSW spot welding of Al-alloy and Mg-alloy sheet materials has indicated that:

1. Tool penetration can be readily explained as a progression of wear events, from mild (delamination) wear through severe wear and finally to melt wear in material beneath the base of the rotating pin. Melt wear can occur under the rotating tool shoulder provided that sufficient penetration of the upper sheet is produced during spot welding.

2. The highest temperatures during FSW spot welding of Al 6111 and AZ91 base materials are close to the solidus temperatures of each base material and correspond with $0.94T_s$ (Al 6111) and $0.99\,T_s$ (AZ91) where T_s is the solidus temperature of the material in degrees Kelvin.

Acknowledgements

The authors wish to acknowledge financial support from the National Science and Engineering Research Council of Canada during this project. They also wish to thank Thixomat of Ann Arbor, Michigan for the supply of the Mg-alloy base material.

References

1. C. SCHILLING, A. VON STROMBECK, J. F. DOS SANTOS and N. VON HEESEN, in Proceedings of the 2nd International Conf. Friction Stir Welding, TWI, June 2000.
2. P.-C. LIN, S.-H. LIN, J. PAN, T. PAN, J. M. NICHOLSON and M. A. GARMAN, SAE Technical Series, 2004-01-1330.
3. O. T. MIDLING and G. RØRVIK, in Proceedings of the 1st International Symposium on Friction Stir Welding, TWI, June 1999.
4. M. RUSSELL and H. R. SHERCLIFF, in Proceedings of the 1st International Symposium on Friction Stir Welding, TWI, June 1999.
5. A. GERLICH, P. SU, T. H. NORTH and G. J. BENDZSAK, in Proceedings of the 3rd Internat. Conf. Advanced Materials Processing, November 2004.
6. A. GERLICH, P. SU, T. H. NORTH, "Magnesium Technology 2005", edited by N. R. Neelameggham, H. I. Kaplan and B. R. Powell (TMS), February 2005.
7. A. GERLICH, P. SU and T. H. NORTH, "Friction Stir Welding and Processing III", edited by K. V. Jata, M. W. Mahoney, R. S. Mishra and T. J. Lienert (TMS), February.
8. P. SU, A. GERLICH and T. H. NORTH, SAE Technical Series 2005-01-1255, in press.
9. J. ZHANG and A. T. ALPAS, *Acta Mater.* **45**(2) (1997) 513.
10. H. CHEN and A. T. ALPAS, *Wear* **246** (2000) 106.
11. Y. LIU, R. ASTHANA and P. ROHATGI, *J. Mat. Sci.* **26** (1991) 99.
12. N. P. SUH "Tribophysics", (Prentice-Hall, Engelwood Cliffs, NJ, 1986).
13. S. C. LIN and M. F. ASHBY, *Acta. Metall.* **25**(1) (1987) 1.
14. P. WANG, J. QU and H. SHAO, in Proceedings of the Internat. Conf. Modeling and Simulation in Metallurgical Engineering and Materials Science, Beijing; June 1996.
15. F. P. BOWDEN and K. E. W. RIDLER, *Proc. Royal Society of London, Series A* **154** (883) (1936) 640.
16. F. P. BOWDEN and P. H. THOMAS, *ibid.* **223** (1152) (1954) 29.
17. T. F. J. QUINN and W. O. WINER, *Wear* **102** (1985) 67.

Received 3 January
and accepted 18 April 2005